Phytolith analysis of late Pleistocene and early Holocene sediments from the Water Canyon Paleoindian site, LA134764, New Mexico

by

Chad L. Yost

Ph.D. Candidate
Department of Geosciences
University of Arizona

Paleoscapes Archaeobotanical Services Team (PAST), LLC

Technical report 16003 prepared for
Robert Dello-Russo
UNM Office of Contract Archeology
Albuquerque, NM

June 2016

Introduction

A total of 16 sediment samples were submitted for phytolith analysis from the Water Canyon Paleoindian site (LA134764), located west of Socorro, New Mexico. The site is located along the eastern edge of the Water Canyon basin, at an elevation of approximately 1760 m (5780 ft), and situated within a juniper savanna ecotone. The phytolith samples are stratigraphic and span a time interval from approximately 14,000 to 9,500 BP. The phytolith samples include sediments from buried wet meadow deposits sometimes referred to as black mats. The goal of this analysis was to determine the presence and abundance of specific types of plants growing at and in the general vicinity of the Water Canyon site based on the recovery of their microscopic silica plant remains called phytoliths. The phytolith extracts also included the silica remains of aquatic organisms, evaporitic minerals, microscopic charcoal and plant starch granules. Together with the phytolith record and other paleoclimate records from the region, this evidence was used to infer general aspects of the climate during the late Pleistocene and early Holocene at the Water Canyon site.

Phytolith Review

Phytoliths are biogenic silica ($SiO_2{-}nH_2O$) in-fillings and casts of cells that are formed in plant tissues such as leaves, stems, bark, fruit and seeds. Phytoliths range in size between 5 and 200 microns, and a single grass plant can produce 10^5 to 10^6 phytoliths (Yost and Blinnikov 2011). When plant matter decays, phytoliths are released and incorporated into soils and sediments. One gram of dry soil can contain 10^4 to 10^6 grass phytoliths (Yost, unpublished data) and one cm^3 of lake sediment can yield 10^4 to 10^5 grass phytoliths (Yost, et al. 2013). Because of their decay-in-place taphonomy, phytoliths tend to represent a very localized vegetation record, whereas pollen records are influenced by both local and regional vegetation. However, depending on the geomorphology of the study area, a proportion of the phytolith record may have been deposited some distance from its initial place of formation due to wind or water transport.

The strength of phytolith analysis lies in its ability to identify grasses (Poaceae) to subfamily and even lower taxonomic levels that require specific temperature and precipitation regimes. Also, grasses are annuals or short-lived perennials whose composition on the landscape can change relatively quickly in response to changes in annual temperature, moisture, light intensity, and land use practices. Because grasses and the phytoliths that they produce are found in virtually every plant community, tracking changes in grass phytolith abundance over time compliments other paleoenvironmental proxies such as pollen and stable isotopes.

The majority of grasses in North America are either members of the Pooideae, Panicoideae or Chloridoideae subfamilies, which produce distinctive and diagnostic phytoliths. Pooideae are cool season mesophytic C_3 grasses that respond favorably to winter precipitation and their abundance on the landscape is negatively correlated with increasing summer temperature (Paruelo and Lauenroth 1996). Panicoideae are warm season mesophytic C_4 grasses that are positively correlated with increasing amounts of summer precipitation. Chloridoideae are

warm season xerophytic C_4 grasses that are positively correlated with increasing summer temperature and decreasing summer precipitation (Taub 2000). Since climate is the dominant control on the distribution of C_3 and C_4 grasses (Huang, et al. 2001), and in particular, the Pooideae, Chloridoideae and Panicoideae subfamilies, reconstructing their proportions on the landscape through the use of phytoliths can reveal changes in temperature and precipitation over time.

Additional Microfossils and Particles in Phytolith Extracts

Although phytolith extraction protocols are optimized for the recovery of biogenic silica from plant cells, other useful microremains and particles are often present in the phytolith fraction recovered from soils and sediments. Some of these microremains recovered in the Water Canyon samples are reviewed next.

Diatoms

Diatoms are single-celled algae with a biogenic silica cell wall. They grow in a wide range of habitats, including the surfaces of wet plants and rocks, damp soils, marshes, wetlands, mudflats, and all types of standing and flowing aquatic habitats (Spaulding, et al. 2010). Their silica cells, or frustules, often are preserved in sedimentary deposits. Because individual taxa have specific requirements and preferences with respect to water chemistry, hydrologic conditions, and substrate characteristics, the presence of diatoms in soils and sediments can provide information about the nature of the local environment or the sources of water used for cooking and food processing.

Freshwater sponges

Freshwater sponges (Porifera: Spongillidae) are primitive members of the animal kingdom. They use biogenic silica to form skeletons comprised of spicules and other structures such as spherasters for support and for reproduction. Freshwater sponges inhabit a wide variety of wet habitats that include ponds, lakes, streams, and rivers; however, they need a hard stratum for growth like submerged logs, aquatic plant stems and rocks. They typically thrive in water that is slightly alkaline (above pH 7), and their abundance is negatively correlated with increasing turbidity, sediment load and salinity. However, some taxa can overcome the negative effects of increasing salinity if calcium ion concentrations are also increasing (Barton and Addis 1997; Cohen 2003; Dröscher and Waringer 2007; Francis, et al. 1982; Harrison 1988).

Chrysophyte stomatocysts

Chrysophyte stomatocysts are biogenic silica structures produced by chrysophycean algae (classes Chrysophyceae and Synurophyceae) during the resting stage of their life cycle (Wilkinson, et al. 2001). Like diatoms, these organisms are often preserved in soils and sediments and can be used to reconstruct past environmental conditions. Chrysophytes are

primarily unicellular or colonial organisms that are abundant in freshwater habitats throughout the world. Chrysophytes are related to diatoms, but are distinct organisms. Chrysophyte stomatocysts are most common in fluctuating freshwater habitats of low to moderate pH and that experience some winter freezing. Many stomatocyst types are found in specific habitats, such as montane lakes, wet meadows, ephemeral ponds, perched bogs, and the moist surfaces of rock and plant substrates. Chrysophyte stomatocysts can also be found in sites that are only wet during certain seasons, such as snowmelt ponds and low swales (Adam and Mahood 1981). In cool-cold temperate lakes, chrysophytes are most common in the spring, when acidic snowmelt dominates the water chemistry. Chrysophytes are intolerant of eutrophic lake conditions (Cohen 2003).

Starch granules

Starch is a plant energy storage substance composed of crystalline and non-crystalline regions made up of amylose and amylopectin. Some of this starch forms globular, spherical, or polyhedral bodies referred to as either grains or granules. Starch granules are found in many plant parts, but are often concentrated in seeds, fruits, roots, and tubers. Starch granules range in size between 1 and 100 microns, and can persist in soil, artifact surfaces, cooking residue and dental calculus for tens of thousands of years. A single plant species often produces a variety of starch granule shapes, sizes and forms. Some of these morphotypes overlap with those produced by other plants; however, there are often morphotypes that are diagnostic of specific plants at various taxonomic levels. When viewed using polarized light microscopy, starch granules appear bright white against a black background, a phenomenon termed birefringence. Chemical extraction, cooking, drying and environmental degradation can result in reduced or even the complete loss of birefringence (Gott, et al. 2006).

Methods

Approximately 6 to 15 grams of sediment from each sample was wet-sieved through a 250-μm mesh and placed in a 400 ml beaker (Table 1). After settling for two hours, the water was decanted. Next, 20 mL of 37% hydrochloric acid (HCl) was added to each sample to remove carbonates and any reaction with the HCl was noted (Table 1). Next, 100 ml of 70% nitric acid (HNO_3) was added to each sample and all samples were heated to 80° C for one hour to oxidize the acid soluble organic fraction. Samples were then rinsed five times with reverse osmosis deionized water (RODI) water. Next, 10 ml of 10% potassium hydroxide (KOH) was mixed into each sample, and after 10 minutes, the solution color was recorded as a qualitative measure of humic acid (humate) content (Table 1). This step was followed by five rinses with RODI water to remove the base soluble organics. Next, a 10% solution of sodium hexametaphosphate was mixed into each sample and the samples were allowed to settle by gravity for one hour, and then decanted to remove any clay-sized particles still in suspension. This step was repeated at least four more times or until the supernatant was clear after one hour of settling. The samples were then transferred to 50 ml centrifuge tubes and dried under vacuum in a desiccator. The dried samples were then mixed with 10 ml of sodium polytungstate (SPT, density 2.3 g/ml) and centrifuged for 10 min at 1,500 rpm to separate the biogenic silica (phytolith) fraction, which

will float, from the heavier inorganic mineral and silica fraction. Each sample was then rinsed five times with RODI water to remove the SPT. Because a significant quantity of platy and low density minerals were extracted along with the phytolith fraction, the samples were re-dried and mixed with a heavy liquid (2.3 g/ml) comprised of cadmium iodide and potassium iodide (CdI_2/KI), which is particularly effective at removing these types of particles. The samples were rinsed five times with RODI and then spiked with polystyrene microspheres for phytolith concentration calculations. The samples were then rinsed twice in 99% ethanol and stored in 1.5 ml vials.

For microscopy, the samples were mounted in optical immersion oil and the cover glass was sealed with fingernail polish. Phytolith counting was conducted with a transmitted light microscope using a magnification of 500x. A minimum of count of 200 taxonomically significant phytoliths was first conducted. Additional phytoliths were counted for samples with high phytolith concentrations to increase the chances of rare phytolith type recovery. Phytolith identification and classification primarily follows Mulholland and Rapp (1992), Fredlund and Tieszen (1994), and Piperno (2006), with morphotype descriptors following the International Code for Phytolith Nomenclature 1.0 (Madella, et al. 2005). For analysis of the results, phytolith relative abundance was based on the phytolith sum. Non-phytolith relative abundances were calculated from the phytolith sum. Phytolith concentrations were calculated from the microsphere counts and normalized to sample sediment weight. Because of the interpretive value, percent relative abundance based only on phytoliths diagnostic of C_3, C_4 xerophytic and C_4 mesophytic grasses was calculated and graphed separately. The 1600 series samples were diagramed separately because they were not dated by the time of this report.

Table 1. Samples analyzed for phytoliths from the Water Canyon site (LA1347640)

FS No.	Test Unit	Level	Modeled Age	Weight started (g)	HCl Rx[†]	KOH Rx[‡]	Phytolith extract (g)	% Phyt.	Extract purity (%)[*]	Phyt conc. (per g)
5005	5-3	1	9,513	6.073	None	Black	0.071	1.169	~99	4,871,283
5059	5-3	2	9,730	6.999	None	Black	0.097	1.386	~99	4,174,439
5095	5-3	4	9,999	6.905	None	Black	0.084	1.217	~95	1,822,940
5123	5-3	6	10,196	7.300	None	Black	0.074	1.014	~98	1,795,518
1195	1-6	9	10,214	6.460	None	Black	0.020	0.310	~98	486,791
1197	1-6	10	10,568	6.505	None	Black	0.024	0.369	~95	991,791
1202	1-6	11	10,956	6.647	None	Black	0.011	0.165	~75	45,133
1203	1-6	12	11,379	6.632	None	Black	0.008	0.121	~50	32,311
1211	1-6	13	11,836	6.987	None	Dk brwn	0.005	0.072	~5	8,419
1217	1-6	14	12,327	6.745	None	Dk brwn	0.005	0.074	< 1	1,186
1219	1-6	15	12,870	14.75	None	Dk brwn	0.008	0.054	< 1	4,676
1229	1-6	16	13,412	7.376	None	Black	0.001	0.014	~5	595
1249	1-6	17	14,006	7.504	None	Black	0.001	0.013	~5	589
1634	1-46	14	TBD	6.294	None	Black	0.002	0.032	~90	6,441
1633	1-46	15	TBD	6.622	Mod	Black	0.002	0.030	~50	1,798
1632	1-46	15	TBD	7.767	None	Dk brwn	0.001	0.013	~25	588

[†] Qualitative observation of sediment reaction in 37% hydrochloric acid (HCl) to estimate $CaCO_3$ content.

[‡] Qualitative observation of sediment reaction in 10% potassium hydroxide (KOH) to estimate humic acid (humate) content; black, brown, and clear correspond to high, moderate, and none.

[*] Extract purity estimated by microscopic examination. Low purity samples often have volcanic glass or low-density evaporites and authigenic minerals such as gypsum and hydrated sodium silicates that could not be removed without losing phytoliths.

Results

Phytoliths

Phytolith preservation varied from good to excellent, and exhibited no evidence for biogenic silica dissolution severe enough to dissolve small and lightly silicified morphotypes. This indicates that changes in the phytolith assemblage reflect coherent changes in the proportionality of C_3 grasses, C_4 grasses, and other plants throughout the entire record (Figures 1 and 2). Phytolith concentrations ranged from a low of 589 per gram (FS 1249) to a high of 4.87×10^6 per gram (FS 5005). Interestingly, phytolith concentrations increased at a near perfect exponential rate from the oldest to the youngest sample. This phenomenon is clearly visible when concentrations were plotted on a log scale (Figure 3 *H*). As is typical, grass and sedge phytoliths comprised nearly 100% of the phytolith record, as trees and shrubs are poor phytolith producers in most temperate biomes. One exception to this was the recovery of a single ponderosa pine (*Pinus ponderosa*) needle phytolith in sample FS 1211 (Figure 4 *U*). With a few exceptions, grass phytolith identifications were limited to the subfamily level, with phytoliths diagnostic of C_4 xerophytic Chloridoideae (Figure 4 *A*, *B*), cool season C_3 Pooideae (Figure 4 *H*, *I*), and C_4 mesophytic Panicoideae (Figure 4 *C*, *D*) generally observed, and listed here, in order of most common to least common. When just considering phytoliths diagnostic of C_3 and C_4 grasses (Figure 3, *A*), C_4 xerophytic (Chloridoideae) grasses dominate much of the record. Interestingly, cool season C_3 grasses are dominant in 3 out of 4 samples between ~11,500 and 10,200 cal BP. This is almost certainly reflective of the dominance of a common wetland C_3 grass such as *Glyceria borealis*, *G. striata or Deschampsia cespitosa* at the site, and not reflective of a switch to C_3 grass dominance in the surrounding uplands. This will be expanded on further in the discussion section.

Lower taxonomic levels of grass identification were made for three taxa. Stipa-type bilobates diagnostic of C_3 subfamily Pooideae, tribe Stipeae grasses were observed throughout the record (Figure 4 *G*). For this location, *Achnatherum* species are the most likely source for this phytolith type. It should ne noted that the genus *Achnatherum* now includes almost all North American grasses formerly included in the *Stipa* (needlegrass) and *Oryzopsis* (ricegrass) genera.

Plateau saddle phytoliths diagnostic of *Phragmites* (common reed, locally as carrizo) were first observed during the Younger Dryas chronozone (YD) in FS 1217 and peaked in abundance in FS 5123 (Figure 4 *J-L*) during the early Holocene. Based on biogeography and the age of these samples, plateau saddle phytoliths are diagnostic of the native *Phragmites australis* ssp. *americanus*, an obligate wetland grass. Today, the native subspecies of *Phragmites* is rare in NM but is listed as occurring in Lincoln, San Juan, and Los Alamos counties; the non-native genotype is listed as occurring throughout New Mexico, including Socorro County (USDA-NRCS 2016). Rondel phytoliths with distinctive angular keels diagnostic of canarygrass (*Phalaris* spp.), an obligate wetland grass, were observed in the early Holocene samples. *Phalaris* first appeared in the phytolith record in FS 1202, which has a modeled age of 10,956 cal BP, and peaks in abundance in FS 1195 (~10,214 cal BP). Both *Phalaris arundinacea* (reed canarygrass) and *Phalaris caroliniana* (Carolina canarygrass) are native to New Mexico, with the former restricted to northern counties and the latter with a more limited and southern

distribution (USDA-NRCS 2016). Based on biogeography and known wetland plant associations, the *Phalaris* phytoliths recovered here are likely derived from *Phalaris arundinacea*. It is very fortuitous that both *Phragmites* and *Phalaris* grasses were identified through their phytolith remains, as these obligate wetland taxa can be used to identify specific wetland plant communities that may be used as modern analogs for the paleowetlands at the Water Canyon site. This approach is expanded in the Discussion section.

Phytoliths diagnostic of sedges (Cyperaceae) were observed in all of the Water Canyon samples and were dominant or codominant with grass phytoliths post-YD until approximately 10,000 cal BP. A phytolith morphotype termed "thin with ridges" derived from sedge leaf, sheath and culm epidermis was the most common sedge phytolith observed (Figure 4 *W*). This morphotype has been observed in a wide variety of genera, including *Scirpus*, *Schoenoplectus* and *Eleocharis* and is likely to be only diagnostic at the family level. The high abundance of this phytolith at times suggests the occurrence of dense stands of sedges. Irregular phytoliths with tubular projections diagnostic of sedge roots and rhizomes were present in low numbers throughout the record and confirm that sedges were rooted at the site (Figure 4 *X*). Three different types of sedge achene cone cells were observed, indicating the presence of at least three sedge taxa. The achene cone cell in Figure 4 *Y* is typical of *Scirpus* and the one in Figure 4 *AA* is typical of *Cyperus*, but similar morphotypes have been observed in other genera such as *Kyllinga* and *Eleocharis*. With some additional modern reference work, it is likely these achene cone cells could be attributed to specific taxa. And lastly, given the high abundance of diagnostic sedge phytoliths in FS 1203 and FS 1202, the highly abundant elongate psilate morphotypes (Figure 4 *T*) attributed to grasses and sedges (Figures 1 and 2) may be predominantly derived from a particular sedge with prolific long cell silicification. Again modern reference work with common New Mexico wetland graminoids may help to identify more taxa.

Evaporite minerals

Some phytolith extracts contained very high concentrations of platy evaporite crystals, particularly those that fall within the Bølling-Allerød chronozone (BA) (Figures 3 *D* and 5 *A*-*B*). By the middle of the YD, evaporite abundance rapidly diminishes. The application of strong acids during phytolith extraction should have removed most of the calcium-based evaporitic minerals such as calcite and gypsum; however, some gypsum may survive exposure to low pH if there has been sodium silicate replacement of the calcium sulfate matrix, which can occur in evaporitic settings with shallow burial depths and sulfate reducing bacteria (Warren 2006). Regardless, the presence of evaporites in the early part of the record is likely due to wind transport from a desiccating basin.

Microcharcoal

Microscopic charcoal was commonly observed in all of the Water Canyon phytolith extracts (Figure 5 *C*). Charcoal particles were counted in two maximum dimension size classes: < 50 μm and > 50 μm, which roughly reflect regionally and locally sourced fires, respectively. Both size classes peak in abundance during the BA and are much reduced during the YD, with the exception of the peak in regional charcoal during the middle of the YD (Figures 3 *C*).

Cryptotephra

Microscopic volcanic glass shards termed cryptotephra were observed in varying amounts in many of the Water Canyon samples (Figure 5 *D*). Subtle cryptotephra peaks were noted in FS 1249 and FS 1217 (Figure 1). Cryptotephra can travel hundreds to several thousands of km from the source eruption. With the advancement of chemical fingerprinting to specific volcanic eruptions, cryptotephra is increasingly being used as an isochron. Of particular interest here is the potential for detection of cryptotephra from the Mount St. Helens (Swift Creek) and Glacier Peak Cascade Range eruptions (13.74-13.45 cal ka BP) that have recently been detected as a cryptotephra couplet in lake sediments from New England (Pyne-O'Donnell, et al. 2016). The cryptotephra observed here should be noted as being a potential isochron if increased sampling resolution and tephra optimized separation techniques are utilized.

Diatoms

Although phytolith extraction techniques are not optimized for diatom recovery, diatoms were observed in every sample except FS 5095 and FS 5123 (Figures 1 and 2). Diatoms were likely in those extracts, but because of high phytolith concentrations, were not observed during the phytolith counts. Pennate diatoms (Figure 6 *C*-*E*) that are typical of shallow water and moist surfaces were rare in the phytolith samples, but most common in the uppermost samples FS 5005 and FS 5059. Centric diatoms such as the two *Aulacoseira* species (Figure 6 *A* and *B*) that are more typically found in rivers, ponds, and lakes were most abundant in the samples from the BA and YD chronozones. *Aulacoseira* abundance (Figure 1) is well correlated with evaporite abundance (Figure 3 *D*) and suggests wind deposition of these diatoms from a desiccating basin. Barbara Winsborough completed a detailed diatom analysis of samples from the same levels as the phytolith samples and presented the results in a separate report (Winsborough 2016).

Freshwater sponges

Microremains from freshwater sponges were present in low numbers and restricted to the late Pleistocene and early Holocene samples (Figure 1). Sponge spicules were highly fragmented (Figure 6 *F*), suggesting eolian transport to site. Sponge spherasters were the most common type of sponge microremain observed (Figure 6 *G*); they peak in abundance during the BA and the first half of the YD. Because of their small size and spherical shape, sponge spherasters may be easily transported along the ground and through the air from desiccating lake basins. Little is known about freshwater sponge ecology, and they are notoriously hard to identify because the reproduction structures needed for identification are rarely observed in sediments. Generally, freshwater sponges thrive in water that is slightly alkaline, and many taxa may be tolerant of some salinity, especially in the presence of calcium ions – conditions typical of some desiccating basins.

Chrysophytes

One chrysophyte stomatocyst was observed in sample FS 5059 (Figure 6 *H*). There were likely many more, however, extremely high phytolith concentrations likely diluted their numbers and reduced their probability of being observed. Chrysophyte algae are understudied, and as

such, their stomatocysts (resting spores) are rarely used as paleoenvironmental indicators. The stomatocyst here corresponds nicely with #270 from the Atlas of Chrysophycean Cysts Vol. II (Wilkinson, et al. 2001), which was collected from a high latitude peat deposit. Progress has been slow in linking stomatocyst morphotypes to the species that produce them; however, finding the same stomatocyst in a modern wetland may help in identifying the type of wetland that existed at Water Canyon during the period of time represented by FS 5059.

Starch granules

Somewhat unexpectedly, 22 starch granules were recovered from FS 1634 and three were recovered from FS 1632 (Figure 2). Starch can survive the phytolith extraction procedure and they are routinely recovered from contexts related to starchy food processing and storage. However, disarticulated granules are not very common in paleoenvironmental contexts, as exposure to water can rapidly gelatinize the granules, making them unrecognizable. Two main types of starch granules were recovered, a faceted polyhedral morphotype with a centric to slightly eccentric hilum (Figure 7 *A*-*F*), and a lenticular morphotype with lamellae visible in plane-polarized light (Figure 7 *G*, *H*). Polyhedral starch granules are produced by a variety of plants, including grass seeds and sedge roots. This particular morphotype is more similar to sedge root types than to grass seed types. An examination of modern sedge roots from taxa commonly found at regional wetland habitats may significantly narrow down the possibilities. The lenticular granules are undoubtedly from C_3 Pooideae tribe Triticeae grass seeds. Based on the work of (Perry and Quigg 2011), their visible lamellae are suggestive of *Pseudoroegneria spicata* (western wheatgrass); however, *Pascopyrum smithii* (western wheatgrass) may also be a possibility for these starch grains if the potential effects of degradation on starch morphology are considered. Modern ambient starch granule contamination is always a possibility; however the recovery of two very different starch morphologies in relatively high abundance from taxa very likely to be growing at or near the Water Canyon site during the study period makes contamination an unlikely source for these granules. It is most likely that a fragment of sedge root and an intact tribe Triticeae grass seed were the source for these starch granules; however, an anthropogenic source is also possible, as grinding activities can easily spread starch granules across a site.

Discussion

Because of its geomorphic setting, the phytolith record from the Water Canyon site is derived from two primary sources, the plants growing in a niche habitat at the site, and plant fragments transported to the site from the surrounding piedmont. Untangling these two sometimes very strong but distinct signals can be a challenge. This is exemplified when viewing the summarized C_3 versus C_4 grass phytolith relative abundance values in Figure 3 *A*. In the southwestern and high plains regions of North America, cool season C_3 grasses are primarily restricted to habitats with high effective moisture such as high elevation sites, riparian zones and wetlands. The C_3 grass signal in Figure 3 *A* is specific to the site, whereas the C_4 mesophytic (Panicoideae) and C_4 xerophytic (Chloridoideae) signal is likely to be exclusively derived from uplands that surround the site and better reflects the dominant grass functional types on the greater landscape. In contrast, phytoliths derived from obligate wetland plants such as sedges

(Cyperaceae), *Phragmites australis*, and *Phalaris* spp. represent a site-specific signal at Water Canyon (Figure 3 *B*). For most of the phytolith record, the landscape signal appears to be dominant and suggests that C_3 grasses and sedges were restricted to the riparian zone along No-Name Arroyo and probably along other drainages in the basin. Between ~11,500 and 10,200 BP, the site-specific signal is dominant, with an expanded wetland comprised of dense grass and sedge vegetation overpowering the greater landscape phytolith signal. For the uppermost four samples with a modeled age range between 10,200 and 9,500 cal BP, it appears that more of a landscape level signal is dominant; however, these four samples are from Locus 5, which is situated on the north side of No-Name Arroyo and in a slightly different geomorphic setting. The high Chloridoideae phytolith abundance may reflect that these grasses were growing at or very close to this location. The shift from Locus 1 samples to Locus 5 samples in the composite phytolith record in part explains the high variability in phytolith abundance values at ~10,200 BP.

It is important to point out that the percent relative abundance of grass functional type phytoliths only approximates their actual proportions in biomass on the landscape. In fact, in modern samples, C_4 xerophytic Chloridoideae phytoliths are often overrepresented when compared to actual Chloridoideae abundance (Blinnikov, et al. 2013; Fredlund and Tieszen 1994). It is also important to point out that both C_4 Panicoideae and Chloridoideae grasses require summer precipitation for growth; however, Chloridoideae grasses decrease in abundance relative to Panicoideae grasses as summer precipitation values increase. For example, between 200 and 400 mm annual precipitation, Chloridoideae grass abundance varies between 60 and 75%, between 600 and 1000 mm this value decreases to around 50%, and above 1000 mm, Chloridoideae values can be as low as 25% (Taub 2000).

Bølling-Allerød Chronozone samples

Samples 1249 (14,006 cal BP) and 1229 (13,412 cal BP) fall securely within the BA. Sample 1219 with its modeled age of 12,870 cal BP and inherent chronological uncertainties is situated on the boundary with the YD (12.9-11.7 ka; Broecker, et al. 2010). The BA warm period spans from 14,700 to 12,900 BP and was interrupted at around 14,000 BP by a brief return to cooler conditions at some Northern Hemisphere locations for a few hundred years. Paleoenvironmental records for the BA are limited in the southwest; however, isotope and packrat midden records from northern Arizona (K. L. Cole and Arundel 2005), and a speleothem isotope record from Fort Stanton Cave in southeastern New Mexico (Asmerom, et al. 2010) indicate warm conditions with variable precipitation during the BA. Lake basin records are also mixed during the BA, with paleolakes Estancia in NM (Allen and Anderson 2000) and Cochise in AZ (Ballenger, et al. 2011) exhibiting evidence for highstands during the first half of the BA, and evidence of regression and desiccation during the second half of the BA. For paleolake San Agustin, the higher elevation C-N sub-basin remained palustrine throughout much of the late Pleistocene; however, the lower elevation Horse Spring sub-basin had regressed significantly and was alkaline by 13,200 BP (Ballenger, et al. 2011).

When considering the phytolith and evaporite records, FS 1219 has a greater affinity to what would be expected for a late BA sample than an early YD sample (Figure 3 *A*). In fact, the rise in C_4 xerophytic phytoliths corresponds with evidence for lake basin desiccation during the

later stages of the BA. Proxies for summer monsoon and tropical cyclone precipitation suggest decreasing intensity as the BA progressed, although still at enhanced levels relative to modern (Antinao and McDonald 2013). Phytolith relative abundance for C_4 mesophytic (Panicoideae) grasses are at their highest levels for the entire record between ~14,000 and 13,500 BP. This is likely due to increased summer precipitation allowing some panicoid grasses to outcompete some C_4 xerophytic grasses. The high values in both local (>50 μm size) and regional (<50 μm size) charcoal (Figure 3 *C*) likely reflects increased fires in late fall or spring due to fuel loading from dried-out summer grass populations and increased lightning activity from summer thunderstorms.

Pollen analysis was conducted on FS 1249 (14,006 cal BP) but only a few grains were recovered (Dello-Russo 2015). The poor pollen preservation was likely due to seasonal wetting and drying. For what was recovered, grass pollen was codominant with Asteraceae, followed by Cheno-am types (Chenopodiaceae family–*Amaranthus* spp.), sage (*Artemisia* spp.) and juniper rounding out the balance of the pollen sum. With the exception of the sedge pollen, there is a paucity of obligate wetland taxa; in fact most of the pollen record is dominated by taxa adapted to seasonal drying. The combined pollen and phytolith data indicates that the Water Canyon site during the BA consisted of a relatively narrow riparian zone lined with C_3 grasses and sedges. The surrounding piedmont consisted of a juniper grassland ecotone comprised of a mix of C_4 mesophytic Panicoideae and C_4 xerophytic Chloridoideae grasses that were supported by higher than modern summer precipitation. Towards the termination of the BA, there may have been a substantial drop in summer precipitation as Panicoideae grass abundance is significantly reduced. The relatively high abundance of C_3 grasses, sedges and tallgrass C_4 Panicoideae may have made the Water Canyon drainage preferable to grazers over lower elevation C_4 shortgrass habitats for much of the BA.

The high evaporite mineral content in BA sediments (Figure 3 *D*), concomitant with the high abundance of both planktonic *Aulacoseira* spp. diatoms and freshwater sponge microremains (Figure 2), suggests that these particles may be an eolian assemblage from a desiccating lake basin. In their reanalysis of the San Agustin Basin cores, Markgraf et al. (1983) did not report the occurrence of *Aulacoseira* diatoms, and explicitly noted the absence of evaporitic minerals. However, the original cores they analyzed appear to have either been recovered from just outside of the lowest elevation sub-basin (Horse Spring Basin) or at the very margin of the sub-basin, and may not be fully representative of the playa conditions. Paleolake Estancia is another potential source for the evaporites and the biogenic silica remains, as there is evidence for a significant desiccation event between ~15,000 and 14,000 BP (Allen and Anderson 2000). Sourcing the origins of the evaporitic minerals at Water Canyon is somewhat tangential but may have relevancy in understanding wind patterns and storm tracts during this portion of the late Pleistocene. The apparent paradox between increased summer precipitation and overall lake basin desiccation during the BA is resolved when considering that winter precipitation is largely responsible for maintaining lake levels, as a significant proportion of summer precipitation can be lost due to evaporation.

Younger Dryas Chronozone samples

The YD spanned from 12,900 to 11,700, as recorded in Greenland ice core $\delta^{18}O$ records (Broecker, et al. 2010). The YD was an abrupt climate change event that affected much of the Northern Hemisphere. Europe experienced significantly cool and wetter conditions, and North America experienced changes in climate that varied by region in both the timing and the direction of change, with some areas experiencing cooler and wetter conditions, while other areas were cooler and dryer (Ballenger, et al. 2011; Carlson 2013; Holliday, et al. 2011). The highest resolution regional paleoclimate record that includes the YD is the Fort Stanton speleothem oxygen isotope record, which is located ~150 km southeast of Water Canyon (Asmerom, et al. 2010). The Fort Stanton speleothem records the YD as a well-defined drop in $\delta^{18}O$ values of 2 to 3‰ (Figure 3 *E*). Speleothem $\delta^{18}O$ values are determined by three variables: 1) precipitation source area, with Pacific Ocean $\delta^{18}O$ values averaging around -11‰, and Gulf of Mexico $\delta^{18}O$ values averaging around -3‰, 2) the amount effect – the more a cloud rains out, the more negative the rain water $\delta^{18}O$ values, and 3) cave and atmospheric air temperature, which equates to about a 0.33‰ speleothem calcite fractionation increase with each degree C increase in air temperature. Thus, the drop in Fort Stanton $\delta^{18}O$ values during the YD is a combination of all three variables; however, based on other paleoenvironmental records, a mostly Pacific (winter) precipitation source and cooler temperatures are the likely cause for the drop in YD $\delta^{18}O$ values at Fort Stanton Cave.

There are numerous regional paleoenvironmental records, including the phytolith record presented here, that indicate a switch from an initially cool and dry YD to a wetter period starting around 12,300 BP. The Scholle wet meadow, located ~100 km northeast of Water Canyon, was active between 12,300 and 11,100 BP (Hall, et al. 2012). Polyak et al. (2004) using speleothem growth rates from the Guadalupe Mountains in southeastern New Mexico conclude that significantly increased precipitation was in place by at least 12,500 BP.

The phytolith record from Water Canyon also is indicative of an initially cool and seasonally dry start to the YD, followed by an increase in precipitation sometime between 12,500 and 12,000 BP. For samples 1217 (~12,327 cal BP) and 1211 (~11,836 cal BP), C_4 mesophytic Panicoideae grass phytoliths rise to ~10% relative abundance, although still lower than during the BA, and C_4 xerophytic Chloridoideae grass phytoliths decrease from 70 to 56% relative abundance. The high relative abundance of C_4 grasses during the late Pleistocene, and in particular during the YD in the Water Canyon samples seems counterintuitive; however, isotopic studies of herbivore teeth from the southwestern US indicate C_4 plant dominance for at least the last 30.0 ka (Connin, et al. 1998). In a carbon isoscape model for North America derived from bison and mammoth tissue $\delta^{13}C$ values, Cotton et al. (2016) reconstruct C_4 grass values of ~40% for the period from 28,000 to 18,000 BP for this part of New Mexico. Interestingly, the boundary with C_4 grass abundance values of 20% or less was modeled to be approximately 100 km from the Water Canyon region. Cotton et al. (2016) also point out that when local changes in temperature do not exceed 8° C lower than modern during the late Pleistocene, C_4 grasses will still be favored over C_3 vegetation due to their greater efficiency with lower atmospheric CO_2 concentrations. Holmgren et al. (2007) using macrofossils from packrat middens propose that temperatures were no more than 5.5° C cooler than today in the Southwest during the late Pleistocene. They go on to speculate that south of 35° N, contiguous C_4 grasslands may have

extended from central Texas to southern Arizona. The landscape level phytolith signal for both the BA and YD at Water Canyon supports this hypothesis.

One *Pinus ponderosa* needle phytolith (Figure 4 *U*) was recovered in sample 1211, indicating the presence of this fire adapted tree within the watershed. C_3 grass phytoliths rise dramatically from 20% to 34% relative abundance in sample 1211. It's important to note that the drop in C_4 xerophytic grass phytoliths is due to both increased C_4 mesophytic grasses at the landscape level (upland grassland) and the rise in C_3 grasses at the site level (wetland/riparian zone). Sedge phytolith abundance is consistent with values during the BA, but the obligate wetland grass *Phragmites australis* ssp. *americanus* (common reed, carrizo) appears for the first time in the record.

Phragmites is an important plant to have a record for because it is a wetland indicator species, and evidence for the presence of a few more indicator plants can be used to identify well-known wetland plant associations and the location of modern analogs. Cattail (*Typha latifolia*) and Baltic rush (*Juncus balticus*) are two such indicator taxa; however, these genera do not produce phytoliths and unfortunately there is no associated pollen record with these samples. However, if the absence of *Typha* pollen for the early Holocene at Water Canyon (Dello-Russo 2015) is extended back to the YD, then the Beaked Sedge Alliance (Muldavin, et al. 2000) (Appendix 1A) may be a potential modern wetland analog for at least the latter half of the YD. Regardless, the presence of *Phragmites* indicates a change from a wet but likely narrow riparian zone to an expanded seasonal wetland with increasingly diverse taxa around 12,300 BP. It's interesting to note the steady increase in the Fort Stanton speleothem $\delta^{18}O$ values throughout the YD, likely due to an increase in the ratio of summer to winter precipitation. It is also interesting to note the spike in the regional charcoal record and its approximate synchronicity with the multidecadal positive excursion in Fort Stanton speleothem $\delta^{18}O$ values just after 12,500 BP.

It appears that at the Water Canyon site, the YD was not expressed as a static climatic event but rather as a transgressive climatic phenomenon. At the onset of the YD, the hydrology was dominated by winter precipitation and summers were relatively dry. With overall cooler temperatures, this may have resulted in greater effective moisture relative to the BA. By the middle of the YD there was a switch to a greater proportion of summer precipitation, however winter precipitation may have been maintained at previous levels, resulting in a net increase in moisture. It's possible that the climatic effects of increasing summer insolation overprinted on the climatic effects of the YD. Numerous climate records have found evidence for a strong link between increasing insolation from changes in the earth's orbital parameters and increased monsoon strength in Africa, Asia, India, and South America, a phenomenon commonly referred to as the orbital monsoon hypothesis (Kutzbach 1981). There have been a limited number of studies that have specifically looked for this same relationship in North America, but evidence is mounting (Anderson 2012; J. E. Cole, et al. 2007; Lachniet, et al. 2013). For the Water Canyon samples, it is intriguing to see the relationship between increasing summer insolation and increasing phytolith concentrations, suggesting a link between grassland densities and summer monsoon intensity in southwestern North America.

Early Holocene samples

Locus 1

Early Holocene samples from Locus 1 have a modeled age range of 11,379 to 10,214 cal BP (FS 1203, 1202, 1197, 1195). This age range includes the period of a summer insolation maximum for July at 30° N, which reaches its peak at around 10,300 BP (Table 2). Use of a 30° N latitude insolation curve is common for investigations of summer monsoons on orbital time scales in Africa and elsewhere; however, the center of action for development of the North American monsoon may be closer to 20° N (Adams and Comrie 1997; Castro, et al. 2001) and perhaps a better fit for investigating a link between increased insolation and monsoon intensity.

Table 2. Peak insolation values and timing for 20° to 40° N Latitude[†]

Latitude for insolation calculation	Peak insolation year (100 year time steps; before year 2000)	Average insolation value for 21 June to 20 July (W/m^2)
20° N	10,500	490.9
25° N	10,400	501.9
30° N	10,300	509.8
35° N	10,200	514.8
40° N	10,100	517.0

[†] Insolation values from Laskar et al. (2004)

The phytolith samples are characterized by a dramatic change in the vegetation signal from the YD record; however, the trends appear to have been initiated during the latter part of the YD. In samples 1203 and 1202, Sedge and C_3 grass phytoliths are overwhelmingly dominant, indicating an expansion of a wetland habitat and an increase in plant densities. C_3 grasses reach their peak in relative abundance in sample 1203. At the landscape level, C_4 grass phytolith abundance values are reduced but this is likely due to the increase in the wetland signal and not reflective of a decrease in C_4 grasses on the surrounding piedmont. Phytoliths from common reed (*Phragmites australis*) reach their second highest value for the record in sample 1203, and reed canarygrass (*Phalaris* cf. *arundinacea*) appears for the first time in sample 1202. It should be noted that both *Phragmites* and *Phalaris* produce a variety of phytolith morphotypes that are not diagnostic; only one type of rondel morphology is diagnostic for these grasses. Thus, these low relative abundance values are significantly underestimating their actual abundance at the site. With several important wetland indicator taxa now identified, comparisons to modern wetland complexes can be made.

The grass and sedge taxa identified in the early Holocene Locus 1 samples key out to the broad category of wetland complexes or alliances termed Persistent Emergent Wetlands by the New Mexico Natural Heritage Program (Muldavin, et al. 2000). Within this broad category are 14 specific alliances that vary from temporarily, seasonally, and semipermanently flooded wetlands along an elevation gradient. With changes in precipitation and temperature over time, paleowetlands likely progressed along varying directions of succession from one type of alliance to another. Assigning the Water Canyon wetland deposits to the persistent emergent wetland

category is fairly secure, but identifying a specific wetland alliance is much more speculative; however, it may be useful in trying to identify modern wetland locations that could be used as analogs for paleowetland deposits such as black mats.

Table 3. Possible modern wetland analogs for Water Canyon paleowetland sediments

Wetland Alliance[†]	Soil type	Redox mottles depth (cm)	Gleyed horizon depth (cm)	Flood recurrence interval (years)	1217	1211	1203	1202	1197	1195	5123	5095	5059	5005
Common Spikerush	Fluvaquent	9.1	20.6	2.6			X	X				X	X	X
Softstem bulrush	Fluvaquent	9.1	20.6	2.6							X			
Reed canarygrass	Mollic Fluvaquent	4.2	18.3	5.2					X	X				
Beaked sedge	Histosol	NP	NP	1.0	X	X	X	X						

[†] Muldavin et al. (2000)

For samples 1203 and 1203, the dominance of sedges and C_3 grasses is consistent with the Beaked Sedge Alliance (Appendix 1A), which may have originated during latter half of the YD. However, associated pollen samples for this period of time indicate the presence of several wetland plants and Asteraceae pollen that suggest an increase in plant diversity, which is consistent with the Common Spikerush Alliance (Muldavin, et al. 2000). Interestingly, birch pollen was recovered in sediments that date between 10,800 and 9,279 cal BP at Water Canyon (Dello-Russo 2015). The modern Scrub-Shrub Wetland complex contains the River Birch (*Betula*) Alliance that includes shrubby maple (*Acer*) and alder (*Alnus*). It seems most likely that that this pollen was transported to the site via wind or water from higher up in the watershed; however, as mentioned in (Dello-Russo 2015), bog birch (*Betula glandulosa*) could have been growing along the margins of the Water Canyon wetland. Although *Betula glandulosa* is not mentioned as being associated with modern emergent herbaceous wetlands (Muldavin, et al. 2000), the unique climatic influences during this period of time likely resulted in some unique plant combinations.

Samples 1197 and 1195 (~10,568-10,215 cal BP) mark the transition to a new dominant wetland plant association. Sedge phytoliths initially drop in relative abundance followed by a rebound, and the appearance of distinctive sedge achene phytoliths similar to those produce by *Scirpus* and *Cyperus* are consistently observed. *Phragmites* phytolith values are unchanged, but *Phalaris* phytoliths reach their highest value for the entire record and general C_3 grass phytoliths reach their second highest value. With values ranging between 500,000 and 1,000,000 phytoliths per gram of sediment, these samples mark the beginning of an explosive rise in phytolith concentrations that eventually peak at almost 5,000,000 in the uppermost sample (FS 5005). A possible modern wetland analog for these samples is the Reed Canarygrass Alliance (Appendix

1C), which can vary from a *Phalaris* monoculture to a rich complex with over 46 wetland graminoids and forbs (Muldavin, et al. 2000). This alliance has dark, anaerobic, mucky, saturated soils that are classified as mollic fluvaquents. Muldavin et al. (2000) note that surface water usually recedes later in the growing season but that the water table remains near the surface. They also note that redox mottles and gleyed horizons form at depths below surface of 4.2 and 18.3 cm, respectively.

Locus 5

The Locus 5 samples examined for phytoliths are FS 5123, 5095, 5059 and 5005. These samples span a modeled age range of ~10,196 to 9,513 cal BP, which includes the waning period of the 30° N summer insolation maximum of 10,300 BP. Despite falling nicely within the increasing phytolith concentration curve, sample 5123 is somewhat of a singularity in regards to its phytolith assemblage. In some respects, it has a strong affinity with the landscape level vegetation signal (C_3/C_4 grasses) for the other 5000 series samples; however, it breaks dramatically with the wetland signal for both the 1100 series samples from Locus 1 and the 5000 series samples. The modeled age for sample 5123 is 10,196 cal BP and the modeled age for sample 1195 is 10,214 cal BP. Based on the uncertainties inherent with an age model and the ^{14}C dates it was based on, these two samples could be contemporaneous or even inverted in relative age. Thus, the jagged shape of the trend line in Figure 3 is not too surprising, especially considering that these loci are on two different sides of No-Name Arroyo and are like recording a different mix of the wetland and landscape vegetation signals.

Regardless of the somewhat peculiar relationship with the samples from either Loci 1 or 5, sample 5123 is recording an interesting wetland signal. Both sedge and *Phragmites* phytolith values are at their highest levels of relative abundance for the record, and C_3 grass phytolith values are still relatively high. This sample may highlight the patchy distribution of wetland plants at the Water Canyon site. The dominance of sedge phytoliths, the relatively high abundance of *Phragmites* and low abundance of *Phalaris* phytoliths suggests an affinity with the Softstem Bulrush Alliance (Muldavin, et al. 2000)(Appendix 1D). This alliance is described as being widespread in New Mexico and characterized by high cover and dominance of softstem rush (*Scirpus tabernaemontani*). Muldavin et al. (2000) describe the soils for this alliance as being anaerobic, dark and poorly drained. They also state that a gleyed mineral horizon typically forms underneath the surface under thick organic accumulations at the surface.

For samples 5095, 5059 and the uppermost sample 5005, obligate wetland indicator grasses and sedges are much reduced, C_3 grasses decline, and C_4 mesophytic and xerophytic grass phytoliths increase in abundance. Despite the apparent reduction in the wetland signal, the phytolith concentration values reach their highest levels for the record. The phytolith assemblages for these three samples are almost a mirror image of the YD samples, yet their phytolith concentrations are over 800 times higher. Also, the humic acid content for these three samples is much higher than for the YD samples (Table 1). The speleothem record from Pink Panther Cave suggests decreasing winter precipitation and overall drying between 10,000 and 9,500 BP (Figure 3 *F*). Increased aridity during this period is also indicated from a soil organic matter $\delta^{13}C$ record from central New Mexico (Hall and Penner 2013). Despite the apparent drying in the region, the Water Canyon site maintained its high water table at least seasonally to

support a very dense grassland community. Seasonal drying may have crossed a threshold where many perennial obligate wetland plants could not remain viable, but C_4 grasses and other herbaceous plants could colonize these areas later in the growing season.

As first discussed in the Results section, a chrysophyte stomatocyst was observed in sample 5059. This stomatocyst corresponds nicely with type #270 from the Atlas of Chrysophycean Cysts Vol. II (Wilkinson, et al. 2001), which was collected from a high latitude peat deposit. The presence of this stomatocyst provides further evidence for the highly organic and acidic conditions of the sediments that the wetland plants were rooted in. Phytoliths are best preserved under slightly acidic conditions, and the phytolith assemblage in this same sample was noted as being perfectly preserved.

The Water Canyon pollen records for this period indicate a high abundance of disturbance taxa such as Cheno-am pollen and a ragweed type pollen that may be derived from marshelder (*Iva* spp.)(Dello-Russo 2012, 2015). Taxa identified from the combined pollen and phytolith records suggest that the Common Spikerush Alliance wetland (Appendix 1B) may be a modern analog for the paleowetland that existed during this period of time. Potential key wetland taxa associated with this alliance type that may be indicated by the pollen and phytolith records include *Cyperus esculentus*, *Eleocharis palustris*, *Helianthus ciliaris*, *Malvella leprosa* and *Iva axillaris* (Muldavin, et al. 2000). This community occurs on sites subject to seasonal flooding, and generally develops as narrow stringers along stream banks with fluvaquent soil development.

1600 Series samples (Locus 1)

At the time of this report, samples 1632, 1633 and 1634 from Locus 1 did not have ages associated with them, so they were not diagrammed as part of the composite record in Figure 3, and instead were diagrammed separately in Figure 2. It was suspected that these samples would fall within the age range of the 1200 series samples (Robert Dello-Russo, personal communication). Comparison to the phytolith record in Figure 1 suggests that these samples may have a chronological affiliation with the 1217 to 1202 set of samples that span from ~12,300 to 10,900 BP.

The most significant finding from these samples was the recovery of 22 starch granules in sample 1634 and 3 starch granules in 1632. Details about these starch granules were discussed in the Results section above, and it was concluded that modern contamination is an unlikely source for these granules. It is most likely that a fragment of sedge root and an intact tribe Triticeae grass seed (for example *Elymus*, *Pascopyrum*, *Pseudoroegneri* or *Hordeum*) were the source for these starch granules; however, an anthropogenic source is also possible, as grinding activities can easily spread starch granules across a site. The probable sedge root starch morphology is consistent with what has been described for *Scirpus tabernaemontani* (syn. *Schoenoplectus tabernaemontani* and *Scirpus validus*) by others (Messner 2011). The previously discussed Softstem Bulrush Alliance, which is dominated by *Scirpus tabernaemontani*, may serve as a modern analog for one of the paleowetland phases at the Water Canyon site.

Conclusion

Phytolith analysis of 16 late Pleistocene and early Holocene samples from the Water Canyon Paleoindian site yielded a well-preserved record of grasses and sedges. The phytolith record consisted of a site level wetland signal comprised of C_3 grasses, obligate wetland grasses and sedges that sometimes overpowered the surrounding landscape signal comprised of C_4 mesophytic (Panicoideae) and C_4 xerophytic (Chloridoideae) grasses.

During the BA, the combined pollen and phytolith data indicates that the Water Canyon site was a relatively narrow riparian zone lined with C_3 grasses and sedges. The surrounding piedmont consisted of a juniper grassland ecotone comprised of a mix of C_4 mesophytic Panicoideae and C_4 xerophytic Chloridoideae grasses that were supported by higher than modern summer precipitation. Towards the termination of the BA, there may have been a substantial drop in summer precipitation as Panicoideae grass abundance was significantly reduced. The relatively high abundance of C_3 grasses, sedges and tallgrass C_4 Panicoideae may have made the Water Canyon drainage preferable to grazers over lower elevation C_4 shortgrass habitats for much of the BA.

The phytolith record suggests that the YD chronozone at the Water Canyon site was not expressed as a static climatic event but rather as a transgressive climatic phenomenon. During the onset of the YD at around 12,900 BP, the phytolith record is indicative of winter-dominated precipitation with low to moderate summer precipitation. By the middle of the YD (~12,300 BP) there was a switch to a greater proportion of summer precipitation, however winter precipitation may have been maintained at previous levels, resulting in a net increase in moisture. It is possible that increased summer insolation resulted in increased monsoon precipitation during the latter part of the YD. Thus, a climate forcing from the progression of the summer insolation maximum may have overprinted on the climatic effects of the waning YD.

For the early Holocene period from ~11,700 to ~10,000 BP, the phytolith record was overwhelming dominated by a sedge and C_3 grass wetland signal. Obligate wetland grasses that included *Phragmites australis* ssp. *americanus* and *Phalaris arundinacea* increased in abundance, and as discussed, may be useful in identifying modern wetland plant alliances that could serve as analogs for the paleowetlands observed at Water Canyon. This period also marked the point where phytolith concentrations increased exponentially, indicative of high grass and sedge densities at the site. This period also brackets the July insolation maximum at 30° N latitude that may have produced a peak in increased summer monsoon precipitation. The relationship between increasing summer insolation and increasing phytolith concentrations at Water Canyon is intriguing, and suggests a link between C_4 grassland densities and summer monsoon intensity in southwestern North America.

For the early Holocene period from ~10,000 to 9,500 BP, obligate wetland indicator grasses and sedges were much reduced, and C_3 grasses declined. The landscape level signal strengthened as C_4 mesophytic and xerophytic grass phytoliths increased in abundance, and phytolith concentration values reach their highest levels for the record, peaking at $\sim 5 \times 10^6$ phytoliths per gram of sediment. This suggests that very dense grasslands dominated the

surrounding landscape, possibly benefiting from enhanced summer monsoon precipitation. However, the reduction in obligate wetland taxa at Water Canyon suggests that winter precipitation was on the decline. The presence of a dense graminoid community consisting of C_3 grasses, sedges and tallgrass C_4 Panicoideae grasses in the Water Canyon drainage likely made this a preferable place for large mammals to graze, especially during the early Holocene.

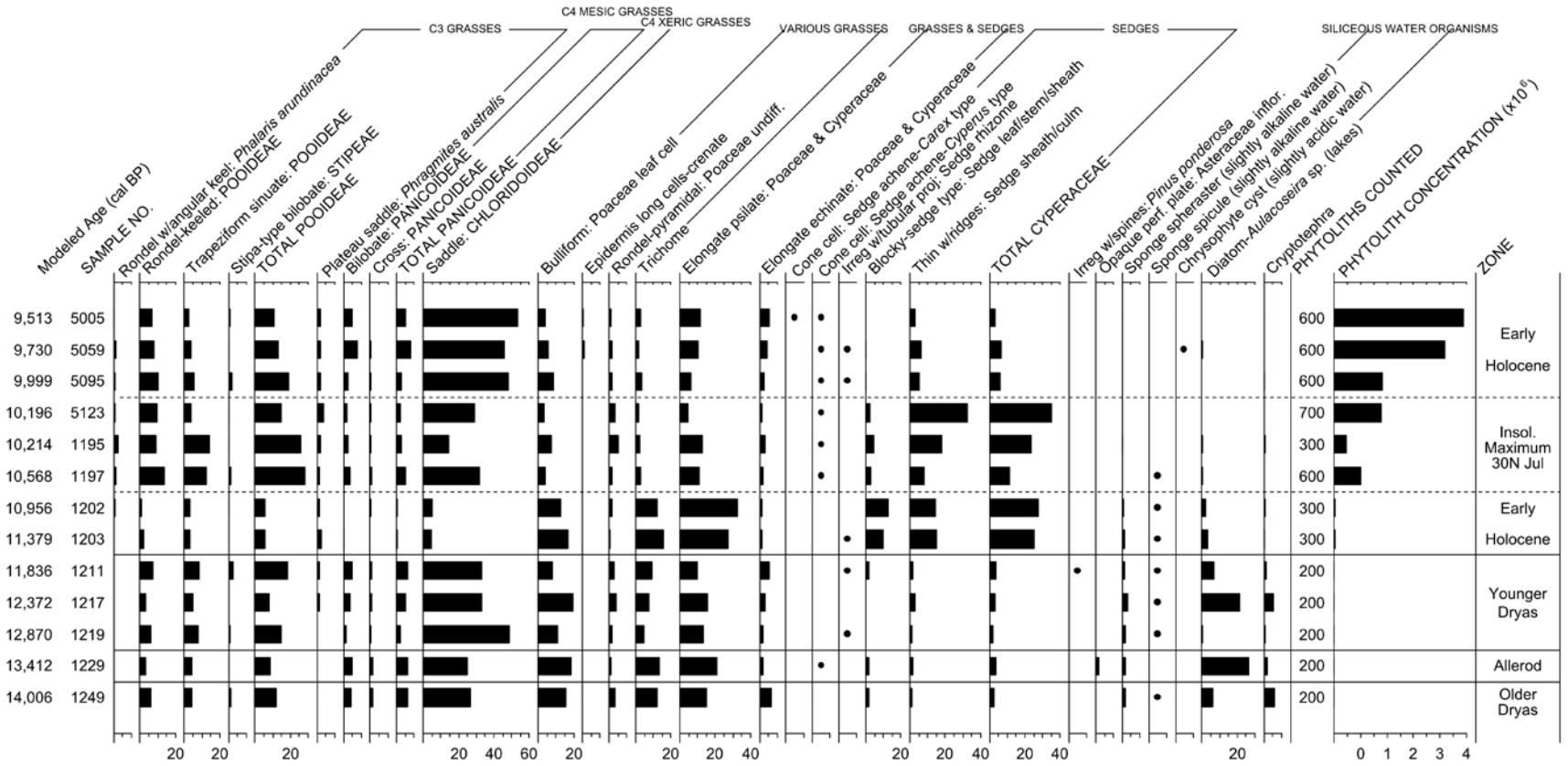

Figure 1. Composite percentage diagram for phytoliths and other siliceous microremains recovered from Loci 1 and 5. Non-phytolith percentages were based on the phytolith sum. Phytolith concentrations were calculated from sediment dry weight.

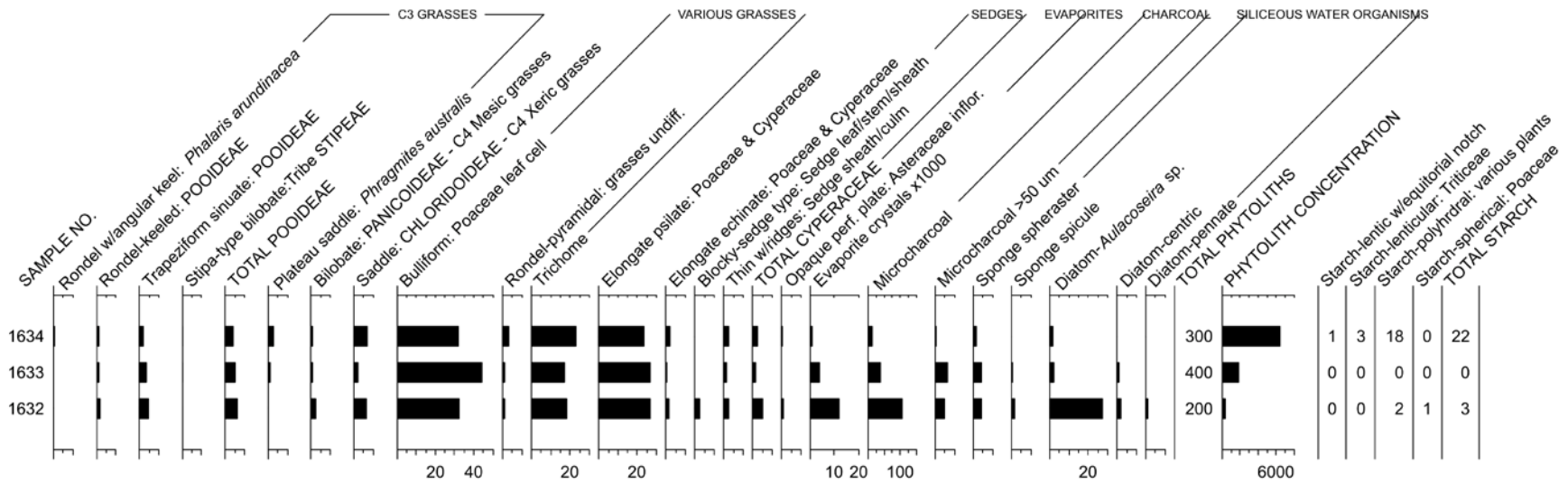

Figure 2. Composite percent relative abundance diagram for phytoliths, charcoal, evaporite crystals and other siliceous microremains recovered from Loci 1, Unit 1-46. Non-phytolith percentages were based on the phytolith sum. Phytolith concentrations were calculated from sediment dry weight. Starch granule values are raw counts.

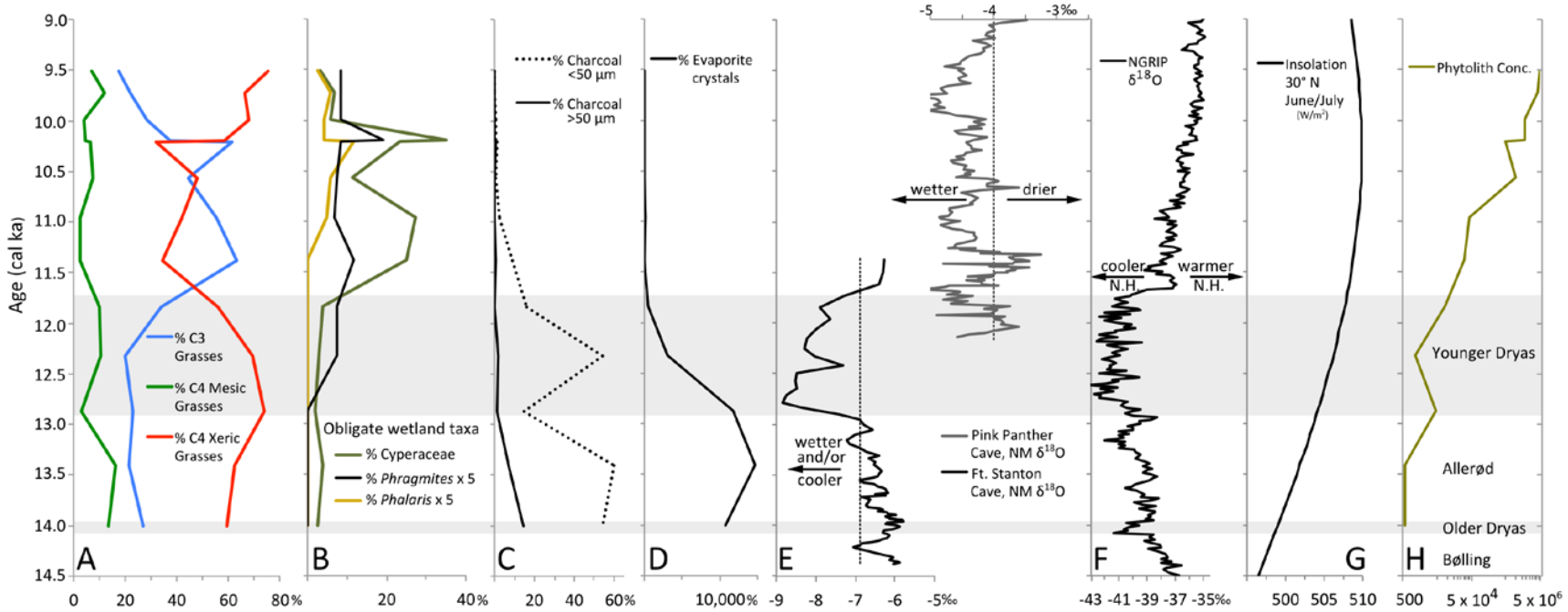

Figure 3. Comparison of select phytolith, microcharcoal and evaporite records from the Water Canyon site to regional and Northern Hemisphere climate records. **A)** Relative abundance values for phytoliths indicative of cool season C_3 grasses, warm season C_4 mesophytic grasses and warm season C_4 xerophytic grasses. The C_3 morphotypes are mostly from subfamily Pooideae taxa, C_4 mesic morphotypes mostly from subfamily Panicoideae taxa, and C_4 xeric morphotypes from subfamily Chloridoideae taxa. **B)** Relative abundance values for phytoliths diagnostic of select obligate wetland grasses (*Phragmites australis* ssp. *americanus*, *Phalaris arundinacea or P. caroliniana*) and sedges (Cyperaceae). **C)** Microcharcoal abundance relative to phytolith sum, with the <50 µm fraction sourced from local and regional fires, and the >50 µm fraction most likely sourced from local fires. **D)** Evaporite crystal abundance relative to phytolith sum, and possibly sourced from the San Agustin basin. **E)** Speleothem oxygen isotope values from Fort Stanton Cave, NM (Asmerom et al., 2007) and Pink Panther Cave, NM (Asmerom et al., 2010). **F)** Greenland oxygen isotope record from the NGRIP core using the GIC05 chronology (Andersen et al., 2007). **G)** Insolation values for June-July at 30° N from Laskar et al., (2004). **H)** Phytolith concentrations per gram dry sediment for grasses (Poaceae) and sedges (Cyperaceae).

Figure 4. Selected phytoliths recovered from Water Canyon site (LA134764) sediments.

All micrographs taken at 500x magnification; scale bar equals 10 μm. **A-B)** Saddle phytoliths derived from C_4 xerophytic grasses (Chloridoideae). **C-D)** Bilobate phytoliths derived from C_4 mesophytic grasses (Panicoideae). **E-F)** Cross phytoliths derived from C_4 mesophytic grasses (Panicoideae). **G)** Stipa-type bilobate phytolith derived from C_3 Pooideae tribe Stipeae grasses. **H)** Keeled rondel phytolith derived from C_3 Pooideae grasses. **I)** Trapeziform sinuate phytolith derive from C_3 Pooideae grasses. **J-L)** Plateau saddle phytolith derived from *Phragmites australis* (common reed), viewed in top, side and oblique positions. **M-O)** Three individual angular keel rondel phytoliths derived from *Phalaris* spp. (canarygrass). **P)** Bulliform cell phytolith derived from grass leaves. **Q)** Part of a silicified grass stomatal complex. **R)** Bulliform-type phytolith typical of grasses (Poaceae) and sedges (Cyperaceae). **S)** Silicified long cell phytolith typical of grasses and sedges. **T)** Elongate-psilate phytolith typical of grasses and sedges. **U)** Irregular with spiny projections phytolith derived from *Pinus ponderosa* needles. **V)** Trichome phytolith typical of grasses. **W)** Thin with ridges phytolith derived from sedge leaf or sheath epidermis. **X)** Irregular with tubular projections phytolith derived from sedge roots and rhizomes. **Y)** Cone cell phytolith derived from sedge achenes, possibly a species of *Scirpus*. **Z)** Sequence of cone cell phytoliths derived from sedge leaf or inflorescence epidermis. **AA)** Cone cell phytolith derived from sedge achenes, possibly from a species of *Cyperus*.

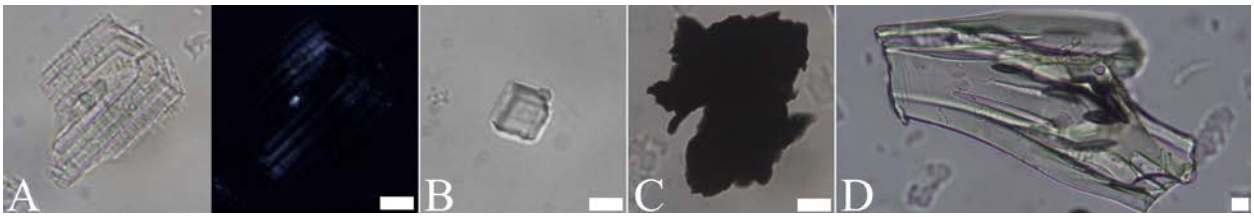

Figure 5. Selected micrographs of evaporite crystals, charcoal and volcanic glass observed in phytolith extracts from Water Canyon site (LA134764) sediments.

All micrographs taken at 500x magnification; scale bar equals 10 μm. **A)** Tabular evaporitic crystal viewed under plane-polarized (left) and cross-polarized light (right). **B)** Rhombic evaporitic crystal. **C)** Microcharcoal particle. **D)** Cryptotephra particle.

Figure 6. Selected micrographs of siliceous water organisms observed in phytolith extracts from Water Canyon site (LA134764) sediments.

All micrographs taken at 500x magnification; scale bar equals 10 μm. Diatom species level identifications were made by Barbara Winsborough. **A)** Two *Aulacoseira* sp. diatom frustules in girdle view. **B)** *Aulacoseira* cf. *italica* diatom in valve view (FS 1633). **C)** *Epithemia adnata* diatom in valve view (FS 5059). **D)** *Surirella* cf. *ovalis* diatom in valve view (FS 5059). **E)** *Stauroneis acuta* diatom in valve view (FS 1632). **F)** Freshwater sponge (Spongillidae) spicule fragment. **G)** Freshwater sponge spheraster. **H)** Chrysophyte (golden algae) stomatocyst (FS 5059).

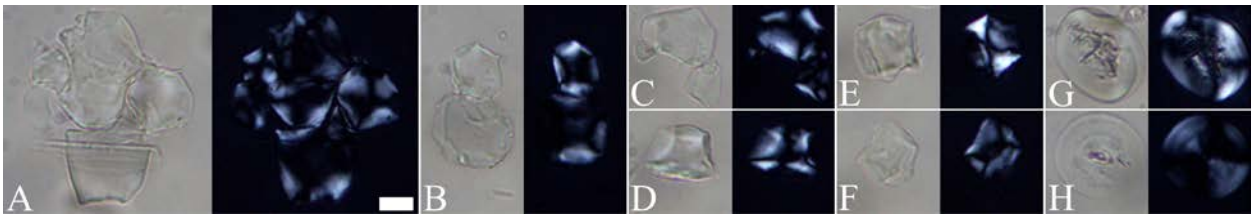

Figure 7. Selected micrographs of starch granules observed in the phytolith extract from Water Canyon site (LA134764) sediment sample FS 1634.

All micrographs taken at 500x magnification with plane-polarized (left) and cross-polarized (right) light; scale bar equals 10 μm. **A-C)** Clusters of faceted polyhedral starch granules. Although some grasses can produce similar morphotypes, these are consistent with those found in sedge (Cyperaceae) roots, in particular *Schoenoplectus*. **D-F)** Individual faceted polyhedral starch granules. **G-H)** Lenticular (in side view) C_3 Pooideae tribe Triticeae granules with visible lamellae under plane-polarized light, characteristics suggestive of *Pseudoroegneri spicata* (bluebunch wheatgrass) seed starch.

References

Adam, David P. and Albert D. Mahood
1981 Chrysophyte cysts and potential environmental indicators. *Geological Society of America Bulletin, Part I* 92:839-844.

Adams, David K and Andrew C Comrie
1997 The North American Monsoon. *Bulletin of the American Meteorological Society* 78(10):2197-2213.

Allen, Bruce D. and Roger Y. Anderson
2000 A continuous, high-resolution record of late Pleistocene climate variability from the Estancia basin, New Mexico. *Geological Society of America Bulletin* 112(9):1444-1458.

Andersen, K. K., M. Bigler, H. B. Clausen, D. Dahl-Jensen, S. J. Johnsen, S. O. Rasmussen, I. Seierstad, J. P. Steffensen, A. Svensson, B. M. Vinther, S. M. Davies, R. Muscheler, F. Parrenin and R. Röthlisberger
2007 A 60 000 year Greenland stratigraphic ice core chronology. *Climate of the Past* 3(6).

Anderson, Lesleigh
2012 Rocky Mountain hydroclimate: Holocene variability and the role of insolation, ENSO, and the North American Monsoon. *Global and Planetary Change* 92-93:198-208.

Antinao, Jose Luis and Eric McDonald
2013 An enhanced role for the Tropical Pacific on the humid Pleistocene–Holocene transition in southwestern North America. *Quaternary Science Reviews* 78:319-341.

Asmerom, Yemane, Victor J. Polyak and Stephen J. Burns
2010 Variable winter moisture in the southwestern United States linked to rapid glacial climate shifts. *Nature Geoscience* 3(2):114-117.

Ballenger, Jesse A. M., Vance T. Holliday, Andrew L. Kowler, William T. Reitze, Mary M. Prasciunas, Shane D. Miller and Jason D. Windingstad
2011 Evidence for Younger Dryas global climate oscillation and human response in the American Southwest. *Quaternary International* 242(2):502-519.

Barton, Susan H. and John S. Addis
1997 Freshwater sponges (Porifera: Spongillidae) of western Montana. *Great Basin Naturalist* 57(2):93-103.

Blinnikov, Mikhail S., Chelsey M. Bagent and Paul E. Reyerson
2013 Phytolith assemblages and opal concentrations from modern soils differentiate temperate grasslands of controlled composition on experimental plots at Cedar Creek, Minnesota. *Quaternary International* 287:101-113.

Broecker, Wallace S., George H. Denton, R. Lawrence Edwards, Hai Cheng, Richard B. Alley and Aaron E. Putnam
2010 Putting the Younger Dryas cold event into context. *Quaternary Science Reviews* 29(9-10):1078-1081.

Carlson, A. E.
2013 The Younger Dryas Climate Event. In *Encyclopedia of Quaternary Science*, edited by S. A. Elias and C. J. Mock, pp. 126-134. Elsevier.

Castro, Christopher L., Thomas B. McKee and Roger A. Pielke
2001 The relationship of the North American monsoon to tropical and North Pacific sea surface temperatures as revealed by observational analyses. *Journal of Climate* 14(24):4449-4473.

Cohen, Andrew S.
2003 *Paleolimnology: The History and Evolution of Lake Systems*. Oxford.

Cole, J.E. , J. Wagner, Jonathan T. Overpeck, J. W. Beck, P. J. Patchett and J. Yang
2007 Holocene hydroclimate of the Sonoran desert: Results from Cave of the Bells, Arizona. *Eos Trans.* AGU, 88(52), Fall Meet. Suppl., Abstract PP13D-01.

Cole, Kenneth L. and Samantha T. Arundel
2005 Carbon isotopes from fossil packrat pellets and elevational movements of Utah agave plants reveal the Younger Dryas cold period in Grand Canyon, Arizona. *Geology* 33(9):713-716.

Connin, Sean L., Julio Betancourt and Jay Quade
1998 Late Pleistocene C4 plant dominance and summer rainfall in the southwestern United States from isotopic study of herbivore teeth. *Quaternary Research* 50(179):179-193.

Cotton, J. M., T. E. Cerling, K. A. Hoppe, T. M. Mosier and C. J. Still
2016 Climate, CO2, and the history of North American grasses since the Last Glacial Maximum. *Science Advances* 2(3):e1501346-e1501346.

Dello-Russo, Robert
2012 *Continued interdisciplinary research at the Water Canyon Paleoindian site (LA 134764), Socorro County, New Mexico: Interim report for the 2010 field season and data reovery plan for the 2012 field season*. Office of Archaeological Studies, Museum of New Mexico, Preliminary Report 42.

2015 *Archaeological excavations at the Water Canyon Paleoindian site (LA 134764), Socorro County, New Mexico: Interim report for the 2012 and 2013 field seasons*. University of New Mexico Office of Contract Archaeology, OCA Report No. 185-1174.

Dröscher, Iris and Johann Waringer
2007 Abundance and microhabitats of freshwater sponges (Spongillidae) in a Danubean floodplain in Austria. *Freshwater Biology* 52(6):998-1008.

Francis, J. C., M. A. Poirrier and R. A. LaBiche
1982 Effects of calcium and salinity on the growth rate of Ephydatia fluviatilis (Porifera: Spongillidae). *Hydrobiologia* 89(3):225-229.

Fredlund, Glen G. and Larry T. Tieszen
1994 Modern phytolith assemblages from the North American Great Plains. *Journal of Biogeography* 21(3):321-335.

Gott, Beth, Huw Barton, Delwen Samuel and Robin Torrence
2006 Biology of Starch. In *Ancient Starch Research*, edited by R. Torrence and H. Barton, pp. 35-45. Left Coast Press, California.

Hall, Stephen A. and William L. Penner
2013 Stable carbon isotopes, C3–C4 vegetation, and 12,800years of climate change in central New Mexico, USA. *Palaeogeography, Palaeoclimatology, Palaeoecology* 369:272-281.

Hall, Stephen A., William L. Penner, Manuel R. Palacios-Fest, Artie L. Metcalf and Susan J. Smith
2012 Cool, wet conditions late in the Younger Dryas in semi-arid New Mexico. *Quaternary Research* 77(1):87-95.

Harrison, Frederick W.
1988 Utilization of freshwater sponges in paleolimnological studies. *Palaeogeography, Palaeoclimatology, Palaeoecology* 62:387-397.

Holliday, Vance T., David J. Meltzer and Rolfe Mandel
2011 Stratigraphy of the Younger Dryas Chronozone and paleoenvironmental implications: Central and Southern Great Plains. *Quaternary International* 242(2):520-533.

Holmgren, Camille A., Jodi Norris and Julio L. Betancourt
2007 Inferences about winter temperatures and summer rains from the late Quaternary record of C4 perennial grasses and C3 desert shrubs in the northern Chihuahuan Desert. *Journal of Quaternary Science* 22(2):141-161.

Huang, Y., F. A. Street-Perrott, S. E. Metcalfe, M. Brenner, M. Moreland and K. H. Freeman
2001 Climate change as the dominant control on glacial-interglacial variations in C3 and C4 plant abundance. *Science* 293(5535):1647-1651.

Kutzbach, J. E.
1981 Monsoon Climate of the Early Holocene: Climate Experiment with the Earth's Orbital Parameters for 9000 Years Ago. *Science* 214(4516):59-61.

Lachniet, M. S., Y. Asmerom, J. P. Bernal, V. J. Polyak and L. Vazquez-Selem
2013 Orbital pacing and ocean circulation-induced collapses of the Mesoamerican monsoon over the past 22,000 y. *Proc Natl Acad Sci U S A* 110(23):9255-9260.

Laskar, J., P. Robutel, F. Joutel, M. Gastineau, A. C. M. Correia and B. Levrard
2004 A long-term numerical solution for the insolation quantities of the Earth. *Astronomy and Astrophysics* 428(1):261-285.

Madella, M., A. Alexandre and T. Ball
2005 International code for phytolith nomenclature 1.0. *Ann Bot* 96(2):253-260.

Markgraf, Vera, J. Platt Bradbury, R. M. Forester, W. McCoy, G. Singh and R. Sternberg
1983 Paleoenvironmental reassessment of the 1.6 million-year-old record from San Agustin Basin, New Mexico. In *New Mexico Geological Society 34th Annual Fall Field Conference Guidebook*, edited by C. E. Chapin and J. F. Callender, pp. 291-297.

Messner, Timothy C.
2011 *Acorns and Bitter roots: starch grain research in the prehistoric Eastern woodlands*. University of Alabama Press.

Muldavin, Esteban, Paula Durkin, Mike Bradley, Mary Stuever and Patricia Mehlhop
2000 *Handbook of Wetland Vegetation Communities of New Mexico*.

Mulholland, Susan C. and George Rapp
1992 A morphological classification of grass silica-bodies. In *Phytolith Systematics*, edited by G. Rapp and S. C. Mulholland, pp. 350. Plenum Press, New York.

Paruelo, Jose M. and W.K. Lauenroth
1996 Relative abundance of plant functional types in grasslands and shrublands of North America. *Ecological Applications* 6(4):1212-1224.

Perry, Linda and J. Michael Quigg
2011 Starch Remains and Stone Boiling in the Texas Panhandle Part II: Identifying Wildrye (Elymus spp.). *Plains Anthropologist* 56(218):109-119.

Piperno, D. R.
2006 *Phytoliths: A comprehensive guide for archaeologists and paleoecologists*. AltaMira Press, Lanham, MD.

Polyak, Victor J., Jessica B. T. Rasmussen and Yemane Asmerom
2004 Prolonged wet period in the southwestern United States through the Younger Dryas. *Geology* 32(1):5.

Pyne-O'Donnell, Sean D. F., Les C. Cwynar, Britta J. L. Jensen, Jessie H. Vincent, Stephen C. Kuehn, Ray Spear and Duane G. Froese
2016 West Coast volcanic ashes provide a new continental-scale Lateglacial isochron. *Quaternary Science Reviews* 142:16-25.

Spaulding, S.A., D.J. Lubinski and M. Potapova
2010 Diatoms of the United States, http://westerndiatoms.colorado.edu.

Taub, Daniel R.
2000 Climate and the U.S. distribution of C4 grass subfamilies and decarboxylation variants of C4 photosynthesis. *American Journal of Botany* 87(8):1211-1215.

USDA-NRCS
2016 The PLANTS Database (http://plants.usda.gov). National Plant Data Team, Greensboro, NC 27401-4901 USA.

Warren, John K.
2006 *Evaporites: Sediments, Resources and Hydrocarbons*. Springer Science and Business.

Wilkinson, A.N., Barbara A. Zeeb and John P. Smol
2001 *Atlas of Chrysophycean Cysts: Vol II*. Springer Netherlands.

Winsborough, Barbara
2016 Diatom analysis at the Water Canyon site NEED CORRECT TITLE

Yost, Chad L. and Mikhail S. Blinnikov
2011 Locally diagnostic phytoliths of wild rice (*Zizania palustris* L.) from Minnesota, USA: comparison to other wetland grasses and usefulness for archaeobotany and paleoecological reconstructions. *Journal of Archaeological Science* 38(8):1977-1991.

Yost, Chad L., Mikhail S. Blinnikov and Matthew L. Julius
2013 Detecting ancient wild rice (*Zizania* spp. L.) using phytoliths: a taphonomic study of modern wild rice in Minnesota (USA) lake sediments. *Journal of Paleolimnology* 49(2):221-236.

Appendix 1

A. Beaked Sedge-Baltic Rush Community Type occurs here in thin bands on the banks of Little Costilla Creek in the upper Rio Grande watershed (from Muldavin et al., 2000).

B. Common Spikerush Alliance on the upper San Francisco River of the Gila River watershed (from Muldavin et al., 2000).

C. Reed Canarygrass Alliance in a marsh along the Rio San Jose in the Rio Grande watershed (from Muldavin et al., 2000).

D. Softstem Bulrush-Broadleaf Cattail Community Type bordering the channel of Oak Creek in the Canadian watershed (from Muldavin et al., 2000).